Dyes and Pigments 83 (2009) 237–248

Contents lists available at ScienceDirect

Dyes and Pigments

journal homepage: www.elsevier.com/locate/dyepig

Analysis of photofading of phenylazo-indole and phenylazo-N-ethanolaniline disperse dyes on poly(ethylene terephthalate) fabric using the PM5 method

Yasuyo Okada [a,*], Toshio Hihara [b], Zenzo Morita [c]

[a] School of Home Economics, Otsuma Women's University, Sanban-cho, Chiyoda-ku, Tokyo 102-8357, Japan
[b] Technical Center, DyStar Japan Ltd., Shinkai-machi 2-65, Omuta, Fukuoka-ken 836-0017, Japan
[c] Tokyo University of Agriculture and Technology, Koganei, Tokyo 184-8588, Japan

ARTICLE INFO

Article history:
Received 27 October 2008
Received in revised form
7 May 2009
Accepted 7 May 2009
Available online 28 May 2009

Keywords:
Disperse dye
Fading of mixture dyeings
Phenylazo-ethanolaniline
Phenylazo-indole
Photo-oxidation
Poly(ethylene terephthalate)

ABSTRACT

The photofading behaviors of phenylazo-N-(ethanol)aniline and phenylazo-indole, nitrohetarylazo-N-substituted aniline disperse dyes on poly(ethylene terephthalate) (PET) substrate were analyzed using the Kubelka-Munk (K/S) parameters of the dyed fabrics exposed to a carbon arc in air. The initial experimental slopes (K_{PET}) of fading on PET were estimated from the time profiles of the K/S values at the λ_{max}. The rates ($k_{0,i}$) of reaction of these dyes with $^1O_2$ were estimated by frontier orbital theory using the PM5 method. The photosensitivities (f_i) of the dyes were estimated from the K_{PET} assuming that the K_{PET} values are proportional to the product of $k_{0,i}$ and f_i. Dyes with small f_i values, irrespective of their $k_{0,i}$ values, possess excellent lightfastness (LF), while dyes with larger f_i values possess poorer LF. The validity of estimating $k_{0,i}$ values by the MO method was confirmed experimentally by analyzing the mutually photosensitized fading behaviors of combination dyeings.

1. Introduction

In a previous paper [1], photo-oxidative fading of disperse azo dyes on poly(ethylene terephthalate) (PET) fabric was confirmed to occur upon exposure to a carbon arc in air. Specifically, we observed the catalytic fading of disperse phenylazo-pyridone dyes, most of which were developed for PET. The rate constants ($k_{0,i}$) of reaction of the azo dyes with $^1O_2$ are estimated by frontier orbital theory using the PM5 method [2]. The fading profiles of disperse azo dyes on PET fabric demonstrate experimentally the validity of the $k_{0,i}$ values calculated by the molecular orbital (MO) method. The photosensitivities (f_i) of six dyes on PET were determined from the slope of photofading based on the assumption that the initial slope (K_{PET}) of oxidative fading is proportional to the product of $k_{0,i}$ and f_i. The photofading behaviors of the dyes on PET can be explained in terms of these two parameters. Dyes with excellent lightfastness (LF) possess small values of both parameters.

When these azo dyes, developed for PET substrate, are applied to nylon 6 (PA) substrate, the LF is estimated to be very low for almost dyes [3] (cf. Table 1). In general, disperse dyes with high or excellent LF on PET, especially dyes with nitro groups, exhibit low LF when applied to PA. The very fast fading on PA is due to photoreduction. Monohydrogenated (MHN) azo dye radicals (a hydrazinyl radical from the azo group or a nitrosyl hydroxide (NOH) radical from the nitro group) are generated by hydrogen abstraction from the substrate in the first step to give a mixture of radical isomers. The MHN radicals engage in a disproportionation reaction: as an H-acceptor the hydrazinyl radicals perform azo scission and the NOH radicals perform the conversion of nitro groups to nitroso groups, and as an H-donor they return to the original dye. The azo scission of the H-acceptor is promoted by the NOH radical of the H-donor as well as by the mutual reaction between hydrazinyl radicals. Since NOH radicals exist at a lower concentration than hydrazinyl radicals, nitrosation is conceived to occur only in limited cases.

On the other hand, some dye manufacturers have tried to synthesize azo and anthraquinone dyes for PA fabric (Procinyl dyes (ICI) as reactive disperse dyes and Resolin P dyes (Bayer) as disperse dyes); their efforts were not successful. Müller reported the structure and LF of disperse dyes on PET and PA at that time

* Corresponding author. Tel.: +81 3 5275 5738; fax: +81 3 5275 7105.
E-mail address: yasuyo.okada@otsuma.ac.jp (Y. Okada).

0143-7208/$ – see front matter © 2009 Elsevier Ltd. All rights reserved.
doi:10.1016/j.dyepig.2009.05.005

Table 1
Photochemical properties of disperse azo dyes examined on PET fabric and their LF on PA fabric.

Dyes	LF	K/S (at λ_{max} [nm])	K_{PET}[a]	$S''_{m,n}(E)$	k/k_{R1}	f/f_{R1}	LF on PA
B3	8	5.59 (457)	0.326_7	0.432	3.63_2	0.216_3	3–4
C1	5–6	6.29 (595)	0.681_2	0.188	0.670_3	2.44_4	1
A3	5–6	12.3 (515)	1.46_5	0.287	1.33_6	2.63_7	4–5
B2	7	8.03 (432)	1.75_7	0.488	5.69_7	0.308_4	6–7
C2	4	1.93 (637)	2.23_0	0.353	2.11_6	2.53_5	1
A2	4	9.14 (489)	2.64_2	0.388	2.74_5	2.31_5	5
B1	6	10.1 (417)	2.93_5	0.475	4.90_3	1.44_0	6
A1	4	6.33 (463)	3.10_9	0.472	4.80_6	1.55_6	5–6
R1 (Red 73)	>6	7.86 (521)	0.415_7	0.245	1.00	1.00	1
E1 (Blue 165)	6	10.5 (629)	0.596_6	0.268	1.17_6	1.22_0	1
D3 (NitropentanoxyCO)	>6	8.04 (444)	0.979_1	0.261	1.10_5	2.13_1	1
E2 (Blue 79:1)[b]	4	6.47 (621)	1.07_5	0.337	1.89_6	1.36_3	1
D4 (Yellow 211)	>6	8.42 (451)	1.14_4	0.249	1.02_2	2.69_2	1
D1 (Yellow 114)	6	10.1 (434)	1.61_1	0.348	2.05_4	1.88_6	1
D5 (MeO2EtOCO)	6	8.20 (447)	1.76_5	0.309	1.56_8	2.70_7	1
E3 (Blue 291)[b]	3	8.69 (643)	2.01_8	0.300	1.46_2	3.32_0	1
D6 (Yellow 241)	5	8.83 (439)	2.03_7	0.276	1.23_3	3.97_4	1
D2 (Quinolone)	4–5	8.19 (437)	3.45_0	0.359	2.18_0	3.80_6	1
E4 (Violet)	2	6.64 (562)	4.52_8	0.413	3.19_4	3.41_0	2–3
D7 (*n*-OctylaminoCO)	4	10.1 (421)	9.37_6	0.219	0.826_9	27.2_7	1

[a] Initial slope of fading on PET ($\times 10^{-6}$ s^{-1}).
[b] The ($k_{0,i}/k_{R1}$, f_i/f_{R1}) values for **E2** and **E3** were revised to be (1.89_6, 1.36_3) and (1.46_2, 3.32_0), respectively, due to the geometry modification.

[4], Kitao et al. [5] examined the effect of *o*- and *p*-nitro groups of the azo dyes on the fading, and Matsuoka et al. [6] extended these reports to LF of the azo dyes. Freeman and Hsu provided a detailed analysis of the photo-decomposed products on PET and PA substrates [7]. However, no decisive conclusion has been attained.

In the present paper, azo dyes with fair or good LF on PA fabric as well as dyes with related chemical structures have been selected. The LF on PET and PA for the dyes used in the present study and reported previously [1,2] are listed, respectively, in the second and last column in Table 1. Irrespective of fair to excellent LF on PET, the most dyes examined previously exhibited very low LF on PA, while dyes selected in the present study fair to good LF on PA except for dyes with nitro group. Besides eliminating nitro groups, what factors result in improving the LF should be interpreted. In order to clarify why they exhibit such low rates of fading on PA, their fading behaviors on PET have been examined applying the same method [1–3]. We intended to confirm whether or not the same rule: (i.e. the rates of fading on PET substrates are expressed by the product of $k_{0,i}$ (the reactivity toward $^1O_2$) and f_i (photosensitivity, or quantum yield to generate $^1O_2$) for the *i*th individual dyes) may be applied to these dyes. We compare values for these dyes with those of a previous study [2] and discuss the fading behaviors of single and mixture dyeings.

2. Experimental

2.1. Dyes used

Eight monoazo disperse dyes, three phenylazo-aniline, two heterocyle-azo-aniline and three phenylazo-indole dyes, were used. In order to examine catalytic fading of these dyes, a yellow pyridone azo dye and a quinolone azo dye were used for diagnostic testing. The numbers of dyes examined previously are listed in Table 1. The chemical structures of the azo (AT) or hydrazone (HT) tautomers of these dyes, which were determined to predominate on the PET substrate (cf. 3.1.1), together with the C.I. generic names, the C.I. constitution numbers (where available), the dominant tautomers, and the dye number (in parentheses) are given as follows.

2.1.1. Azo dyes from N-ethanolanilines

1) An azo dye from monoethanolamine, AT

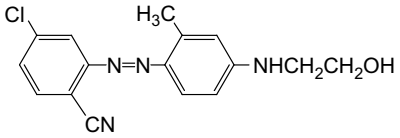

(A1)

2) An azo dye from bis(ethanol)amine, AT

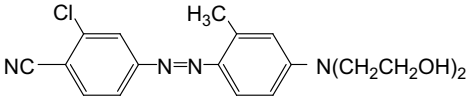

(A2)

3) An azo dye from acetylamino-bis(ethanol)amine, AT

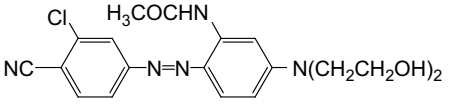

(A3)

2.1.2. Azo dyes from indoles

1) An azo dye from methylindole, AT

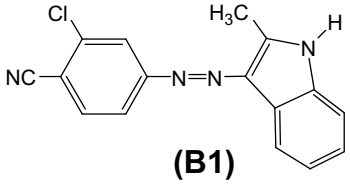

(B1)

2) An azo dye from phenylindole, AT

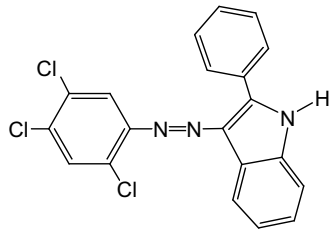

(B2)

3) An azo dye dichloronitrophenylazo-phenylindole, AT

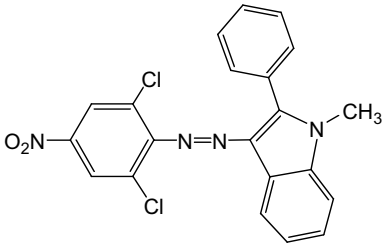

(B3)

2.1.3. Azo dyes from heterocyclic diazo components

1) C.I. Disperse Blue 148, C.I. 11 124, AT

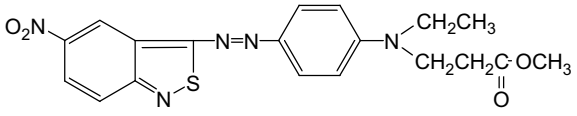

(C1)

2) A 5-nitrothiazole azo dye, AT

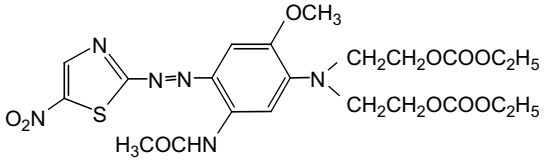

(C2)

2.1.4. Yellow dyes for diagnostic testing

1) C.I. Disperse Yellow 114, C.I. 128 455, HT

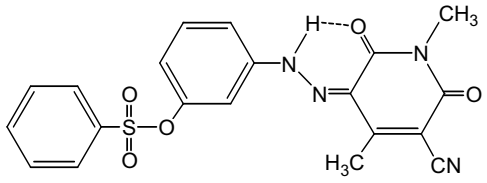

(D1)

2) A quinolone azo dye, HTs, (General number: **D2**)

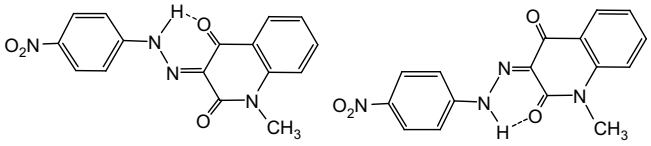

A-type of HT (HT-A) B-type of HT (HT-B)

2.1.5. Materials and methods for dyeing and exposure

The PET fabric used was double-pique grade F1142 (dtex/filament: 84/36, weight: 240 g/m^2; Toray Industries). The dyeing was carried out by the same method as before [1,2].

The dyed fabrics were exposed to a carbon arc by a fadeometer (Suga Test Instruments). The reflectance spectra of the dyed and exposed fabrics were measured using a V-550 UV–vis spectrophotometer equipped with an integrating sphere (Jasco Ltd). The K/S values at the λ_{max} of the original singly-dyed PET fabrics are listed in Table 1. (In order to examine the absorption at wavelengths $<$ 400 nm especially for yellow dyes, the reflectance spectra 250–780 nm were measured. The K/S spectra of dyes on substrate were obtained by subtracting the K/S spectra of undyed fabric from those of the dyed fabric. PET has strong absorption (λ_{max} = ca. 300 nm) and is not transparent $<$ 320 nm. But since some existence of decomposed products is seen in the spectra at the wavelengths $<$ 280 nm, all the K/S spectra 250–780 nm are illustrated in the figures.)

2.2. Molecular orbital calculations

All the MO calculations were carried out using CAChe MOPAC 2002 (Windows edition, version 6.1.12.33) (Fujitsu). For the ATs and HTs of the eight dyes in the gaseous and aqueous phases, structure optimization was performed to derive the molecular parameters, which included the standard heats of formation [$\Delta_f H^0$(gas) and $\Delta_f H^0$(H_2O) (kcal mol^{-1}), in the gaseous and aqueous phases, respectively], the energies of HOMO and LUMO (E_{HOMO} and E_{LUMO}, respectively), the electron densities in HOMO (d_{HOMO}), the electrophilic frontier densities ($f_r^{(E)}$), and the dipole moment (μ) in the gaseous phase, using the PM5 method. The COSMO method was used to calculate the parameters in the aqueous phase.

3. Results and discussion

3.1. Analyses using the PM5 method

3.1.1. Azo-hydrazone tautomerism (AHT)

Only dyes **A3** and **C2** can exhibit AHT, while the other dyes exist only as ATs. The $\Delta_f H^0$(gas) and $\Delta_f H^0$(H_2O) values for the ATs and HTs of the two dyes are listed in Table 2. For dyes **A3** and **C2**, both values for the ATs are lower than those for the HTs, indicating that both dyes exist as ATs. In this paper, only the properties of ATs are discussed, since both dyes can be regarded as existing as ATs on PET substrate.

3.1.2. Reactivities toward $^1O_2$ in terms of electrophilic frontier electron density

The $^1O_2$ adds to the double bonds in aromatic molecules via [2 + 2] and [4 + 2] cycloadditions or the ene reaction, all of which belong to pericyclic reactions. ([4 + 2] Cycloaddition was excluded, since it was reversible and performed no decomposition.) More

than one double bond which possesses reactivity towards $^1O_2$ exists in a dye molecule. These reactions sometimes compete with each other [8]. For disperse azo dyes on PET [1,2] and many series of reactive azo dyes on cellulose [9–15], we found good correlations between the rates of oxidative fading and the sum, $S^{(E)}_{m,n}$, of the $f^{(E)}_r$ at the two adjacent atomic positions defined by:

$$S^{(E)}_{m,n} = \sum_{m,n}\left\{f^{(E)}_m + f^{(E)}_n\right\}, \quad (1)$$

where $f^{(E)}_r$ denotes the frontier electron density for the electrophilic reaction type, which is the weighted sum of the squares of the coefficients of the LCAO MO according to frontier orbital theory [16–19]. The $S^{(E)}_{m,n}$ values correspond to the sum of reactivities of the double bonds in a dye molecule towards $^1O_2$ or the reactivity of photo-oxidation for the dye.

3.1.3. Estimation of $S^{(E)}_{m,n}$ values

Applying the same procedure to the present disperse azo dyes as in previous studies [1,2,9–15], the $S^{(E)}_{m,n}$ values of the ATs for the eight azo dyes examined were estimated as shown in Table 2. Without estimating the $\Delta_f H^0$(gas) values for the reaction intermediates and end-products of the ATs for the eight dyes, the reactivity of individual double bonds toward $^1O_2$ was estimated in terms of $f^{(E)}_r$. In order to check the validity of the estimation, the electron densities of HOMO, d_{HOMO}, are also listed in Table 3.

1) ***Dyes A1, A2, and A3***: All the atomic sites in the coupling component except for C6 contribute to the reactivity (cf. Table 2). The contributions from the double bond of C9═C10 and the atomic site of C6 are excluded due to the small d_{HOMO} values at C9, C10 and C6 as shown in Table 3. The double bond of N7═N8 may be excluded due to its very high energy of formation [10–13]. As a result, double bonds with high reactivities toward $^1O_2$ exist only in the phenyl ring of the coupling component.
2) ***Dyes B1 and B3***: Only the double bonds of C1═C2 and C15═C16 contribute to the reactivity, resulting in intermediate $k_{i,0}$ values and a small f_i value. Contributions by the double bonds of C4═C6 and C17═C18 are excluded due to the small d_{HOMO} values at C6 (0.010 − 0.008) and C17 (0.015 − 0.019) (the former values correspond to dye **B1**), respectively, as shown in Table 3.
3) ***Dye B2***: The same situations hold for the double bonds of C1═C2 and C15═C16. Contributions from the double bond of C17═C18 are excluded due to the small d_{HOMO} value at C17 (0.007), while the contribution at C4 is taken into consideration due to the large d_{HOMO} value at C4 (0.033), compared with the d_{HOMO} values at C4 for dyes **B1** and **B3** (Table 3). The double bond of N7═N8 may be excluded due to its very high energy of formation, as above [10–13]. As for the reactivities of the three indole dyes, the double bonds having potential reactivity toward $^1O_2$ are: C1═C2, C15═C16, and C15═C4 (for dye **B2** only) in the indole ring.
4) ***Dye C1***: Only the double bonds C3═C4 and C4═C5 in the coupling component contribute to the reactivity. The double bonds C1═C2, C6═C1, and N7═N8 may be excluded due to the small d_{HOMO} values at C2 (0.012), C6 (0.016) and N7 (0.009). No contributions of the double bonds in the diazo component are considered due to the small d_{HOMO} values (Table 3).
5) ***Dye C2***: The double bonds C1═C2 and C4═C5 in the coupling component contribute to the reactivity. There is no contribution from the double bonds C9═N13, C1═C6 and N7═N8 due to the small d_{HOMO} values at C9 (0.000), C6 (0.015) and N7 (0.003), respectively (Table 3).

Thus, in the case of the two hetarylazo dyes, double bonds with reactivities toward $^1O_2$ are found in the phenyl ring of the coupling component.

3.1.4. Estimation of $S''_{m,n}(E)$ values

Since the disperse azo dyes used in this study were comprised of diazo and coupling components with a wide range of chemical structures, one should take into consideration not only the effect of the orbital energy differences between the dye and $^1O_2$ but also the effect of the electron densities in the HOMO. Thus, a first approximation of the electrophilic superdelocalizability can given as follows [2,16–19]:

Table 2
Enthalpy of formation, $\Delta_f H^0$(gas) and $\Delta_f H^0(H_2O)$ (kcal mol^{-1}) in gas and aqueous phase, dipole moment, μ (debye), HOMO and LUMO energies, for azo and hydrazone tautomers of yellow azo dyes in the gas phase, and electrophilic frontier density, $f^{(E)}_r$, for the most probable tautomer, estimated by semiempirical MO PM5 method.

Dye	**A1**	**A2**	**A3**		**B1**	**B2**	**B3**	**C1**	**C2**	
M.W.	314.774	358.827	401.852		294.743	400.694	425.273	413.450	568.557	
	AT	AT	AT	HT	AT	AT	AT	AT	AT	HT
$\Delta_f H^0$(gas)	62.557	22.491	−13.157	−7.301	127.324	116.489	125.790	35.447	−234.998	−214.322
μ	5.299	3.168	2.543	10.354	6.193	3.289	8.436	7.065	7.541	11.224
E_{HOMO}	−8.742	−8.792	−9.184	−8.833	−8.541	−8.505	−8.585	−8.991	−8.970	−9.214
E_{LUMO}	−1.149	−1.313	−1.619	−1.659	−1.116	−0.860	−1.784	−2.047	−2.447	−2.025
$\Delta_f H^0(H_2O)$	45.211	3.401	−40.529	−32.376	112.819	104.711	109.262	12.955	−271.355	−251.872
$f^{(E)}_r$(site) for the most	AT	AT	AT		AT	AT	AT	AT	AT	
probable tautomer	0.401 (C1)	0.315 (C1)	0.225 (C1)		0.437 (C1)	0.338 (C1)	0.416 (C1)	0.149 (C3)	0.254 (C1)	
	0.074 (C2)	0.075 (C2)	0.101 (C2)		0.205 (C2)	0.235 (C2)	0.167 (C2)	0.144 (C4)	0.156 (C2)	
	0.155 (C3)	0.133 (C3)	0.109 (C3)		0.166(C15)	0.114 (C4)	0.166(C15)	0.174 (C5)	0.161 (C4)	
	0.187 (C4)	0.164 (C4)	0.155 (C4)		0.157(C16)	0.145(C15)	0.147(C16)		0.297 (C5)	
	0.237 (C5)	0.199 (C5)	0.177 (C5)			0.142(C16)				
								0.274 (C1)		
					0.073 (C6)		0.076 (C6)	0.027 (C2)	0.055 (C6)	
	0.042 (C9)	0.037 (C9)	0.034 (C9)		0.108 (C4)	0.085 (C6)	0.105 (C4)	0.033 (C6)	0.006 (C9)	
	0.034(C10)	0.027(C10)	0.017(C10)		0.096(C17)	0.164(C18)	0.102(C17)	0.070 (C9)	0.004(N13)	
	0.040 (C6)	0.030 (C6)	0.059 (C6)		0.193(C18)	0.098(C17)	0.186(C18)	0.031(C17)	0.010 (N7)	
	0.053 (N7)	0.048 (N7)	0.064 (N7)			0.045 (C9)		0.026 (N7)	0.067 (N8)	
	0.097 (N8)	0.072 (N8)	0.030 (N8)			0.024(C10)		0.085 (N8)		
						0.007(C14)		0.046(C15)		
								0.033(C16)		
$S^{(E)}_{m,n}$	1.054	0.886	0.767		0.965	0.974	0.896	0.467	0.868	
$S''_{m,n}(E)$	0.472	0.388	0.287		0.475	0.488	0.432	0.188	0.353	

Table 3
Electron densities of HOMO, d_{HOMO}, for phenylazo-aniline and heterocyclic azo-aniline disperse dyes.

	A1[a]	A2[b]	A3[c]		C1[d]		C2[e]		B1[f]	B2[g]	B3[h]
	AT	AT	AT		AT		AT		AT	AT	AT
C1	0.222	0.174	0.141	C1	0.175	C1	0.146	C1	0.275	0.240	0.276
C2	0.033	0.033	0.032	C2	0.012	C2	0.081	C2	0.111	0.155	0.086
C3	0.075	0.063	0.029	C3	0.093	C3	0.006	N3	0.109	0.085	0.133
C4	0.105	0.092	0.101	C4	0.095	C4	0.092	C4	0.024	0.033	0.022
C5	0.125	0.104	0.092	C5	0.110	C5	0.170	–	–	–	–
C6	0.015	0.009	0.016	C6	0.016	C6	0.015	C6	0.010	0.021	0.008
N7	0.024	0.021	0.034	N7	0.009	N7	0.003	N7	0.026	0.043	0.022
N8	0.046	0.033	0.013	N8	0.036	N8	0.036	N8	0.069	0.022	0.064
C9	0.012	0.010	0.011	C9	0.002	C9	0.000	C9	0.012	0.012	0.007
C10	0.007	0.005	0.000	S10	0.001	S10	0.007	C10	0.012	0.000	0.004
C11	0.002	0.000	0.000	N11	0.000	C11	0.003	C11	0.001	0.001	0.001
C12	0.006	0.003	0.000	C12	0.001	C12	0.000	C12	0.010	0.000	0.000
C13	0.000	0.000	0.000	C13	0.000	N13	0.001	C13	0.002	0.001	0.000
C14	0.005	0.003	0.000	C14	0.000	N14	0.192	C14	0.004	0.003	0.001
N15	0.252	0.292	0.303	C15	0.000	N15	0.057	C15	0.095	0.082	0.100
				C16	0.000			C16	0.084	0.091	0.081
				C17	0.003			C17	0.015	0.007	0.019
				N18	0.335			C18	0.117	0.108	0.121

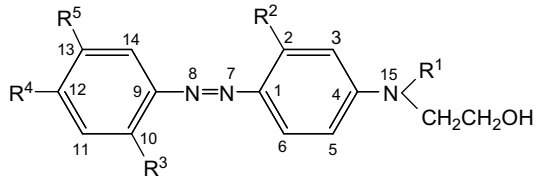

[a] $R^1 = H$, $R^2 = CH_3$, $R^3 = CN$, $R^4 = H$, $R^5 = Cl$.
[b] $R^1 = CH_2CH_2OH$, $R^2 = CH_3$, $R^3 = H$, $R^4 = CN$, $R^5 = Cl$.
[c] $R^1 = CH_2CH_2OH$, $R^2 = NHCOCH_3$, $R^3 = H$, $R^4 = CN$, $R^5 = Cl$.

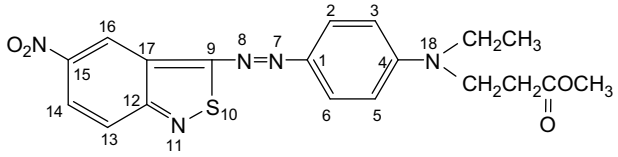

[d] As set.

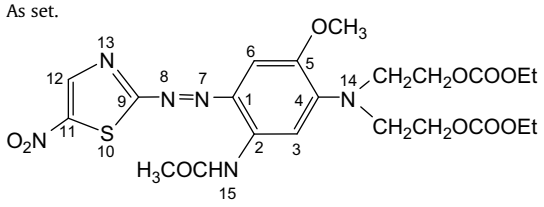

[e] As set.

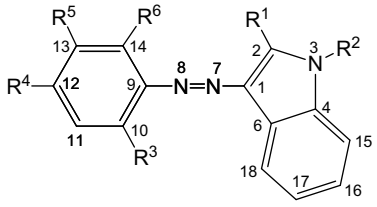

[f] $R^1 = CH_3$, $R^2 = R^3 = R^6 = H$, $R^4 = CN$, $R^5 = Cl$.
[g] $R^1 = Phenyl$, $R^2 = R^3 = R^4 = R^5 = Cl$, $R^6 = H$.
[h] $R^1 = Phenyl$, $R^2 = CH_3$, $R^3 = R^6 = Cl$, $R^4 = NO_2$, $R^5 = H$.

$$S''_{m,n}(E) = \frac{S^{(E)}_{m,n}(-\beta)}{E^{^1O_2}_{LUMO} - E^{Dye}_{HOMO}}, \quad (2)$$

where β is multiplied to make it dimensionless (−1.0 eV). The contribution of the electrons in the orbitals with lower energies than the HOMO in the dye molecule to the reactivity is taken into consideration in Eq. (1), while the contribution of the orbital energy difference between the dye and $^1O_2$ is taken into consideration only by the denominator of Eq. (2). The $S''_{m,n}(E)$ values for the eight dyes are listed in Table 2. The orders of the $S^{(E)}_{m,n}$ and $S''_{m,n}(E)$ values for the eight dyes are considerably different, indicating that double bonds with $f_r^{(E)}$ values (electron density) and E_{HOMO} values (energy level) determine the reactivities towards $^1O_2$, which are given by frontier orbital theory [16–19]. The reactivities cannot be analyzed according to simple substituent effects.

As examined in previous papers [1,2], smaller $S^{(E)}_{m,n}$ values result in lower reactivity toward $^1O_2$. Among twenty dyes, including

twelve dyes examined previously, dyes **A3** and **C1** exhibited the smallest $S''^{(E)}_{m,n}$ values (cf. Tables 1 and 2). These two dyes possess the lowest E_{HOMO} values, which produces lower $S''_{m,n}(E)$ values or reactivities towards $^1O_2$. Although **C1**, a hetarylazo dye developed for PET, possesses the lowest $S''_{m,n}(E)$ values, dye **A3**, exhibiting a limiting property among the six dyes examined, does not possess excellent photochemical properties on PET like the other five dyes. (This fact is experimentally demonstrated below.)

3.2. Photofading of singly-dyed PET fabric

Plotting ln $(KSR)_t/(KSR)_0$ (the logarithms of the relatively reduced values of K/S at the λ_{max} after exposure) against the time of exposure, the initial rates of fading, K_{PET}, for the eight azo dyes were estimated from the slopes of the plots. The K_{PET} values are listed in Table 1 in ascending order. The disperse azo dyes used have a wide range of hues. As mentioned in previous papers [1,2], yellow dyes possess high LF irrespective of relatively larger K_{PET} values, while red and blue dyes have rather low LF irrespective of smaller K_{PET} values, since human color vision is most sensitive to red hues and least sensitive to yellow hues.

When a second-order reaction occurs between the *i*th azo dye (D_i) and $^1O_2$ with an assumed rate constant of $k_{0,i}$ (mol^{-1} kg s^{-1}), the equation for the second–order reaction is described in terms of the following steady-state approximation:

$$-\frac{d[D_i]}{dt} = k_{0,i}[^1O_2][D_i], \quad (3)$$

where *t* is the time of reaction. The sensitization of the *i*th dye in the single dyeings is given by:

$$[^1O_2] = [^3O_2]f_i \quad (4)$$

Since $[^1O_2]$ is kept constant during the initial period of irradiation, the reaction of the dye with $^1O_2$ may be regarded as being of pseudo-first-order. Integrating Eq. (3), the initial slope of fading is given as follows:

$$\lim_{t\to 0}\{\ln[(KSR)_0/(KSR)_t]/t\} = K_{PET}, \quad (5)$$

From Eqs. (3)–(5), it may be shown that K_{PET} is proportional to the product of $k_{0,i}$ and f_i (i.e., $K_{PET} = k_{0,i}[^3O_2]f_i$).

3.2.1. K_{PET} and f_i/f_{R1} values from single PET dyeings

Using the linear relationship between the $S''_{m,n}(E)$ values and ln $k_{0,i}$ (the hypothetical values and the reference value of dye **R1**), whose validity was demonstrated in previous studies [2,10–14], the relative values of $k_{0,i}/k_{R1}$ are estimated as listed in Table 1. From the K_{PET} and $k_{0,i}/k_{R1}$ values, the relative values of f_i/f_{R1} are also estimated. The order of K_{PET} and $k_{0,i}/k_{R1}$ and the range of the values or ratings for f_i/f_{R1} and LF are summarized in Table 4. As a whole, those dyes with small f_i/f_{R1} values possess high LF, while those with rather large f_i/f_{R1} values have a lower LF. However, large $k_{0,i}/k_{R1}$ values do not always result in low LF, as LF depends also on the hue or on the sensitivity of human color vision [1,2].

Dyes **B1** and **B2** possess better LF, irrespective of larger K_{PET} values, than the red and blue dyes. When dye **B3** is applied to single dyeings of PET, it behaves like dyes with super LF because no properties based on large $k_{0,i}/k_{R1}$ values are exhibited due to the very small f_i/f_{R1} values. It possesses the same property which perspiration-light-fast dyes, such as azo dyes derived from γ-acid, have [12]. Substituting a nitro group for the chloride in the diazo component of **B2** lowers the electron density of HOMO at the C4 site or decreases the $k_{0,i}/k_{R1}$ values which results in a decrease in the f_i/f_{R1} values as well, although no reason for the decrease in the latter could be found.

Table 4
Analyses of photofading of phenylazo-aniline and -indole dyes on PET fabric upon exposure to a carbon arc in air.[a]

Dye	K_{PET}		Order or range		
	Relative values	Order[b,c]	$k_{0,i}$[d]	f_i[e]	LF[f]
B3	0.8	1	6	a	a
C1	1.6	3	1	c	b
A3	3.5	4	3	c	b
B2	4.2	5	9	a	a
C2	5.4	6	4	c	c
A2	6.4	7	5	c	c
B1	7.1	8	8	b	b
A1	7.5	9	7	b	c
R1	1.00	2	2	a	a

[a] cf. Table 1.
[b] For order, larger number describes larger rates or values.
[c] The same order as that of relative values of $f\,k_0$, which have the same values as the rates of fading for single PET dyeings.
[d] Estimated by MO method (cf. Tables 1 and 2).
[e] Range of f_i^e: a = equal or smaller than that of Red 73, *b* = 1.4–1.6, *c* = 2.3–2.6.
[f] Range of LF: a ≥ 7, *b* = 5–6 – 6, *c* = 4.

When the two terms, $k_{0,i}/k_{R1}$ and f_i/f_{R1}, are compared among the three indole dyes, f_i/f_{R1} values decrease in the order: **B1** > **B2** > **B3**, corresponding to an increase in the quantum yield of internal conversion. Although N-methyl and/or 2-phenyl groups in the indole may be responsible for this efficiency, further elucidation is required. It is noted that a double bond with reactivity towards $^1O_2$ exists in the ring of both the diazo and the coupling components, although dyes other than the indole azo dyes possess the double bonds only in the coupling components.

Among the three azo dyes derived from N-ethanolanilines, the order of $k_{0,i}/k_{R1}$ values was: **A1** > **A2** > **A3**. Although the primary change in electron density in HOMO is attributed to the $f_r^{(E)}$ values in the phenyl ring of the coupling component, and primarily to the values at the C1 site, no substituent effects responsible for the change can be proposed.

Dye **C1** from the hetaryl diazo component possesses good LF, while **C2** has only fair LF. Although these dyes have nearly similar f_i/f_{R1} values, the LF of **C1** is higher than that of **C2** due to its much smaller $k_{0,i}/k_{R1}$ value. It is noted that the double bonds bearing reactivity towards $^1O_2$ exist in the coupling components of the two hetarylazo dyes. Thus, the hetaryl diazo component itself has little effect on their reactivity but rather on their hue.

The correlations between LF and two terms indicated the same features in these dyes including the other disperse dyes examined previously [2], although no structural characteristics were extracted.

3.3. Mutually photosensitized fading in the mixture dyeings

As was the case in previous papers [1,2], the Kubelka-Munk K/S parameters at the λ_{max} of each dye from the reflectance spectra of exposed fabrics were used to estimate the fading of the individual dyes in the combination dyeings. Since little absorption of yellow dyes occurs at the λ_{max} of blue dyes and weak absorption of blue dyes occurs at the λ_{max} of yellow dyes, the original K/S values of the yellow dyes, $(K/S)_{Original}$, were reduced by the corresponding values overlapping the real values to K/S_{Red} (cf. Tables 5–7). Plotting ln $(KSR)_t/(KSR)_0$ against the time of exposure, the rates of fading for the seven yellow dyes were estimated from the slopes of the plots, as listed in Table 5 (combination dyeing with **A3**), Table 6 (combination with **E1**) and Table 7 (combination with **C1**).

In the case of **A3** in combination with the two yellow dyes, the absorption spectra of the component dyes overlapped each other at both values of λ_{max}. In order to avoid superposition of the absorption spectra, the absorptions at 530 nm and 515 nm (λ_{max}) were used for **A3** in the mixture dyeing with **D2** and **D1**, respectively, at which

Table 5
Reactivity ratios determined by Eq. (6) using the Kubelka–Munk parameters for **A3** in mixture dyeings with **D2** and **D1** and the rates of fading in single dyeings.

Dye (λ_{max})	Mixture dyeing								
	Time (h)	**D2** (437 nm)			Dye examined		$k_{0,Yellow}/k_{0,A3}$		
		K/S_{Orig}	K/S_{Red}	KSR[a]	K/S	KSR[a]	Each expos.	Aver.	by MO
A3[c] (515 nm)	0	9.577	8.184						
	20	8.264	7.011	0.857					
	40	7.417	6.227	0.761					
	60	6.114	5.127	0.626					
	0				4.671			1.5_2	1.6
	20				4.205	0.900	1.47		
	40				3.992	0.855	1.75		
	60				3.312	0.709	1.36		
	λ (nm)[b]				530				
		D1 (434 nm)			Dye examined				
	Time (h)	K/S_{Orig}	K/S_{Red}	KSR[a]	K/S	KSR[a]	Each expos.	Aver.	by MO
A3 (515 nm)	0	7.223	3.837		12.432			1.1_5	1.5
	20	6.452	3.380	0.881	11.283	0.908	1.31		
	40	5.855	3.045	0.793	10.319	0.830	1.24		
	80	5.019	2.710	0.706	8.482	0.682	0.91		

Single dyeing

	Time (h)	K/S_{Orig}	KSR[a]		Time (h)	K/S_{Orig}	KSR[a]
A1 (463 nm)	0	6.333		**C1** (595 nm)	0	6.293	
	20	4.393	0.694		20	5.995	0.962
	40	3.972	0.627		40	5.923	0.941
	80	2.682	0.424		80	5.163	0.820
A2 (489 nm)	0	9.143		**D1** (434 nm)	0	10.087	
	20	7.184	0.786		20	8.849	0.877
	40	6.341	0.694		40	8.227	0.816
	80	4.476	0.490		60	7.140	0.708
A3 (515 nm)	0	12.268		**D2** (437 nm)	0	8.193	
	20	10.976	0.895		20	6.050	0.738
	40	10.062	0.828		40	4.943	0.603
	80	8.028	0.654		60	3.939	0.481
B1 (417 nm)	0	10.107		**D4** (451 nm)	0	7.975	
	20	8.785	0.869		20	7.247	0.909
	40	7.412	0.733		40	6.842	0.858
	80	5.499	0.544		60	6.362	0.798
B2 (432 nm)	0	8.030		**D7** (421 nm)	0	10.061	
	20	6.772	0.843		20	6.797	0.676
	40	6.185	0.770		40	4.119	0.409
	80	4.907	0.611		60	2.595	0.258
B3 (457 nm)	0	5.593		**E1** (629 nm)	0	10.396	
	20	5.536	0.990		20	9.582	0.922
	40	5.339	0.954		40	9.427	0.909
	80	5.088	0.910		60	9.359	0.900

[a] K/S ratio = KSR = $(K/S)_t/(K/S)_0$.
[b] Wavelength used to avoid the superposition of reflectance spectra.
[c] The K/S values in the lower row for **A3** in the mixture dyeing with **D2** are the corresponding K/S_{Red} values.

wavelengths there was little absorption by the yellow dyes, while absorption at the λ_{max} was used for each yellow dye (cf. Table 5). Since the light absorption of **D1** at 515 nm is negligible, the rates of fading for **A3** in the mixture dyeings were estimated by the absorption at 515 nm. Since the light absorption of **D2** at 515 nm is not negligible, however, the rates of fading for **A3** in the mixture dyeings with **D2** were estimated by the absorption at 530 nm. The overlapping of the absorption spectra of **A3** and the yellow dye was estimated at the wavelengths listed above. From the K/S ratios, $(KSR)_t$, at time t of exposure at the wavelengths of individual dyes, as explained above, the ratios of $k_{0,i}$ for the component dyes in the various binary combination dyeings are given by [2]:

$$\frac{k_{0,i}}{k_{0,j}} = \frac{\ln\frac{[D_{t,i}]}{[D_{0,i}]}}{\ln\frac{[D_{t,j}]}{[D_{t,j}]}} = \frac{\ln\left[(KSR)_t/(KSR)_0\right]_i}{\ln\left[(KSR)_t/(KSR)_0\right]_j}, \quad (6)$$

and are listed in Tables 5–7

In the mixture dyeing of **E1** with the pyridone azo dyes [1,2], the yellow dyes apparently suppressed the rate of fading for **E1**, but the $k_{0,Yellow}/k_{0,E1}$ observed varied with each dye, although they were in some agreement with theoretical values. In the present study, however, as explained below, the $k_{0,i}/k_{0,A3}$ values obtained from the combination dyeings of **A3** were identical to those estimated by MO theory, while some of the $k_{0,i}/k_{0,C1}$ values were identical and all the $k_{0,i}/k_{0,E1}$ values were not. The reason why the fading behaviors of some mixture dyeings deviate from the behaviors described by the theoretical values is discussed.

3.3.1. *Mixture dyeings with **A3***

In the mixture dyeing with **D2**, the rate of fading for **A3** is slightly decreased, compared with those in the single dyeings, while that for **D2** is considerably decreased (cf. Table 5). The K/S spectra of their mixture dyeings upon light exposure indicate a considerable fading of both dyes irrespective of the severe mutual overlap of their spectra as illustrated in Fig. 1. The observed $k_{0,i}/k_{0,A3}$

Table 6
Reactivity ratios for seven dyes by Eq. (6) using Kubelka–Munk parameters from the mixture dyeing with **E1** and the other blue dyes.

Dye	Time (h)	Mixture dyeing					$k_{0,Yellow}/k_{0,E1}$		
		Yellow dye			E1(629 nm)		Each expos.	Aver.	by MO
		K/S_{Orig}	K/S_{Red}	KSR	K/S	KSR			
A1 (463 nm)	0	3.082	2.587		10.487			16.4	4.1
	10	2.081	1.583	0.612	10.537	0.980	24.3		
	20	1.681	1.196	0.463	9.839	0.960	18.9		
	40	1.534	1.069	0.413	10.260	0.938	13.8		
A2 (489 nm)	0	5.318	4.558		10.593			12.9	2.3
	10	4.640	3.873	0.850	10.698	0.990	16.2		
	20	4.227	3.478	0.783	10.450	0.982	13.5		
	40	4.043	3.303	0.725	10.316	0.974	12.2		
A3 (515 nm)	0	6.377	5.073		10.403			11.5	1.1
	10	5.841	4.552	0.897	10.283	0.988	9.0		
	20	5.453	4.163	0.821	10.290	0.984	12.2		
	40	5.100	3.824	0.754	10.180	0.979	13.3		
B1 (417 nm)	0	4.652	4.125		10.531			14.1	4.2
	10	3.600	3.078	0.662	10.283	0.980	21.5		
	20	2.738	2.213	0.536	10.331	0.958	14.5		
	40	2.149	1.649	0.400	9.844	0.935	13.6		
B2 (432 nm)	0	3.736	3.222		10.593			10.4	4.8
	10	3.580	3.072	0.953	10.698	0.990	16.2		
	20	3.200	2.691	0.835	10.450	0.982	13.5		
	40	2.862	2.360	0.732	10.316	0.974	12.2		
B3 (457 nm)	0	2.637	2.171		10.357			0.53	3.1
	20	2.624	2.161	0.995	10.285	0.993	0.71		
	40	2.598	2.156	0.990	10.069	0.980	0.50		
	80	2.608	2.145	0.988	10.035	0.969	0.38		
D4 (451 nm)	0	8.450	8.006		10.160			2.4_6	0.9
	20	7.927	7.495	0.936	9.875	0.972	2.32_8		
	40	7.212	6.792	0.848	9.593	0.944	2.86_0		
	60	6.843	6.440	0.804	9.210	0.906	2.21_0		

Mixture dyeing of **E1** with yellow dye

Yellow partner dye	$k_{0,Yellow}/k_{0,E1}$ [1]		Yellow partner dye	$k_{0,Yellow}/k_{0,E1}$ [1]	
	Obsd.	MO		Obsd.	MO
D1	7.1	1.7	**D5**	6.7	1.3
D2	8.3	1.9	**D6**	5.1	1.0
D3	2.8	0.9	**D7**	9.6	0.7

Mixture dyeing of blue dye with **D1**

Blue component dye	$k_{0,D1}/k_{0,Blue}$ [2]		Partner dye	$k_{0,D1}/k_{0,Blue}$ [2]	
	Obsd.	MO		Obsd.	MO
E2	1.7	1.1	**E4**	0.48	0.6
E3	1.2	1.4	**R1**	3.6	2.1

Mixture dyeing of blue dye with **D2**

Blue component dye	$k_{0,D2}/k_{0,Blue}$ [2]		Partner dye	$k_{0,D2}/k_{0,Blue}$ [2]	
	Obsd.	MO		Obsd.	MO
E1	8.6	1.9	**E4**	0.92	0.7
E2	4.6	1.1	**R1**	6.2	2.2
E3	3.0	1.5			

Table 7
Reactivity ratios for four dyes determined by Eq. (6) using Kubelka–Munk parameters from the mixture dyeing with **C1**.

Dye	Time (h)	Mixture dyeing					$k_{0,Yellow}/k_{0,C1}$		
		Yellow dye			**C1**(595 nm)		Each expos.	Aver.	by MO
		K/S_{Orig}	K/S_{Red}	KSR	K/S	KSR			
D1 (434 nm)	0	4.683	4.087		6.147			2.3_8	3.1
	20	4.286	3.727	0.912	5.896	0.959	2.24		
	40	4.049	3.503	0.857	5.759	0.937	2.37		
	60	3.498	2.972	0.727	5.422	0.882	2.54		
D2 (437 nm)	0	8.843	8.251		6.256			3.4_0	3.2
	20	7.496	6.931	0.840	5.980	0.956	3.87		
	40	6.687	6.144	0.745	5.742	0.918	3.44		
	60	6.353	5.508	0.667	5.443	0.870	2.90		
D4 (451 nm)	0	8.560	7.871		6.382			0.93_7	1.5
	20	7.948	7.312	0.929	5.886	0.922	0.906		
	40	7.734	7.113	0.904	5.745	0.900	0.957		
	60	7.304	6.720	0.854	5.404	0.847	0.950		
D7 (421 nm)	0	10.776	10.071		6.343			3.2_4	1.2
	20	8.618	7.969	0.791	5.841	0.921	2.88		
	40	7.534	6.911	0.686	5.602	0.883	3.02		
	60	6.023	5.422	0.538	5.400	0.851	3.84		

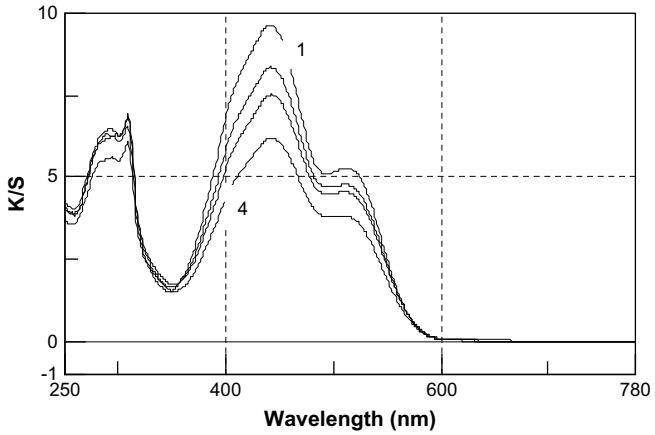

Fig. 1. K/S spectra of mixture-dyed PET with dyes **A3** and **D2** on exposure to a carbon arc for: 1, 0 h; 2, 20 h; 3, 40 h and 4, 60 h (Spectra 2 and 3 (from top to bottom) in sequence are illustrated between 1 and 4.).

values coincided very well with the theoretical values by the PM5 method, indicating that the two dyes shared $^1O_2$ between them according to the simple rate law described by Eq. (6) (cf. Table 5).

In the mixture dyeing with **D1**, both the rates of fading for **A3** and **D1** were considerably lowered, compared with those in the single dyeings (cf., Table 5 and Fig. 2). The observed $k_{0,i}/k_{0,A3}$ value for **D1** is a little smaller than the theoretical one.

The K/S spectra of the two component dyes overlap considerably with each other as shown in Figs. 1 and 2. The two dyes in the mixture dyeings upon light exposure exhibited similar fading behaviors. Thus, the validity of $k_{0,i}$ values estimated by the MO method was experimentally demonstrated almost completely utilizing the mutual photosensitizing effects in the mixture dyeings with admixture of **A3** with **D1** and **D2**. These dyes displayed their own properties described by the two $k_{0,Yellow}/k_{0,A3}$ and f_i/f_{R1} parameters. The theoretical $k_{0,Yellow}/k_{0,A3}$ values were confirmed to be identical with the experimental values through Eq. (6), a complete description of the fading behaviors in the mixture dyeings in terms of two parameters irrespective of spectral overlapping, although the mixture dyeing with E1 exhibited a considerable shift between the theoretical and experimental values [1]. This is discussed below.

3.3.2. Combination dyeings of *E1*

Fading behaviors of mixture dyeings with **E1** were described by the theoretical $k_{0,Yellow}/k_{0,E1}$ values (determined by the MO method) and the experimental f_i/f_{R1} values (obtained in the single dyeings), although the behaviors were modified by the partner dyes [1,2]. The modification or the shift in the $k_{0,Yellow}/k_{0,E1}$ values described by Eq. (6) was attributed to the superposition of the absorption spectra of the component dyes and the f_i/f_{R1} values of the partner dye. Since phenylazo-pyridone dyes possess the narrow main absorption band (MAB) of yellow, the effects of spectral overlap by the yellow dyes over the blue dye were considerably limited. Phenylazo-N-ethanolaniline and phenylazo-indole dyes that have a MAB with considerable overlap over the blue dyes may yield useful information about the spectral overlap effect.

Phenylazo-indole and phenylazo-aniline dyes, however, seemed to suffer marked catalytic fading (although this fading behavior may not be called catalytic even if it is very different fading from that of single dyeings) or mutually photosensitized (or photosensitization-effect noticeable) fading by **E1** and partner dyes. This indicates larger experimental $k_{0,Yellow}/k_{0,E1}$ values, $(k_{0,Yellow}/k_{0,E1})_{Exp}$, than the theoretical values, $(k_{0,Yellow}/k_{0,E1})_{MO}$, except for **B3**. The ratio of the observed to theoretical values depended upon the extent of spectral overlapping described by the λ_{max} of the partner dyes as follows (cf. Table 6):

$$\left[(k_{0,Yellow}/k_{0,E1})_{Exp}/(k_{0,Yellow}/k_{0,E1})_{MO};\lambda_{max}(\text{partner dye(s)})\right]:$$
$$[10.5;515\,\text{nm}(\mathbf{A3})] > [5.6;489\,\text{nm}(\mathbf{A2})] > [4.0;463\,\text{nm}(\mathbf{A1})]$$
$$> [\leqq 3.4;\leqq 451\,\text{nm}(\mathbf{B1},\mathbf{B2},\mathbf{D3}\,\text{and}\,\mathbf{D4})]. \quad (7)$$

The closer the λ_{max} of the partner dye to that of **E1** or the larger the spectral overlap, the larger the ratios, indicating an effect of spectral overlap. The rates of fading for **E1** in the mixture dyeings were considerably smaller than those in the single dyeings. The behaviors are illustrated in Fig. 3 along with their spectral overlapping. At the shorter wavelengths, **E1** possesses strong absorption which causes generation of $^1O_2$. When the absorption responsible for the sensitization was partially shielded by the spectral overlap, the generation of $^1O_2$ by the sensitization by **E1** was to a corresponding extent suppressed, which lowered the fading of **E1** to a larger extent than that of the partner dye. (This was probably due to the heterogeneous distribution of dyes in the solid polymer, which is enhanced with further fading.)

Phenylazo-pyridone dyes exhibited a photosensitization-noticeable tendency [1,2] in the mixture dyeings with **E1**. As in the case of **C1** (cf., Sec. 3.3.3), when the ratios: $(k_{0,Yellow}/k_{0,E1})_{Exp}/(k_{0,Yellow}/k_{0,E1})_{MO}$; λ_{max} (partner dye); and f_i/f_{R1}) are calculated, they become as follows:

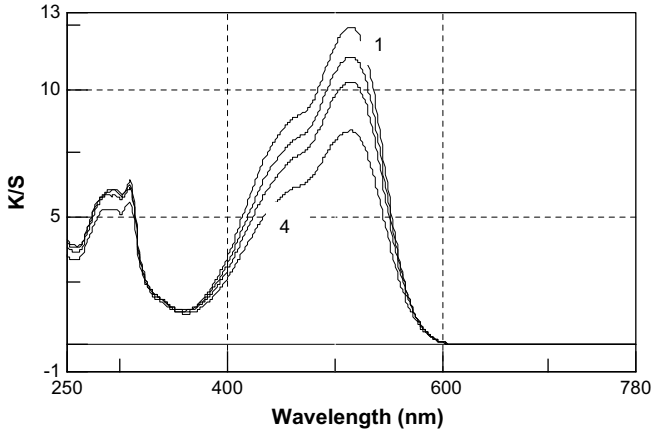

Fig. 2. K/S spectra of mixture-dyed PET with dyes **A3** and **D1** on exposure to a carbon arc for: 1, 0 h; 2, 20 h; 3, 40 h and 4, 60 h (Spectra 2 and 3 (from top to bottom) in sequence are illustrated between 1 and 4.).

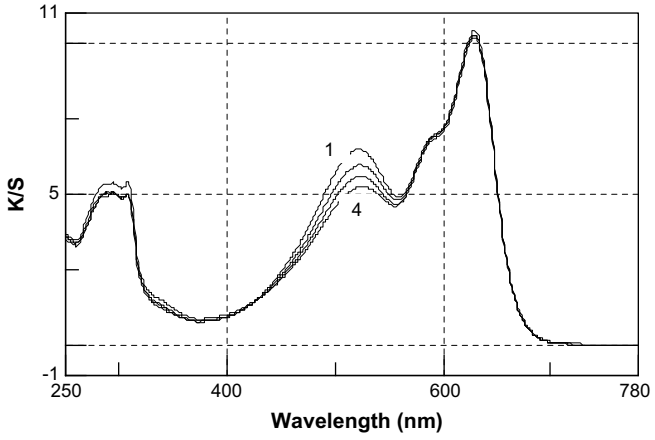

Fig. 3. K/S spectra of mixture-dyed PET with dyes **A3** and **E1** on exposure to carbon arc in air for: 1, 0 h; 2, 10 h; 3, 20 h; and 4, 40 h. (Spectra 2 and 3 (from top to bottom) in sequence are illustrated between 1 and 4.).

$$\left[(k_{0,\mathrm{Yellow}}/k_{0,\mathrm{E1}})_{\mathrm{Exp}}/(k_{0,\mathrm{Yellow}}/k_{0,\mathrm{E1}})_{\mathrm{MO}};\lambda_{\max}(\text{partner dye});(f_i/f_{\mathrm{R1}})\right] : [13.7;421\ \mathrm{nm}](\mathbf{D7};27) > [5.2;440\ \mathrm{nm}(\mathbf{D5};2.7)]>[5.1;438\ \mathrm{nm}(\mathbf{D6};4.0)]>[4.5;437\ \mathrm{nm}(\mathbf{D2};3.8)] > [4.2;434\ \mathrm{nm}(\mathbf{D1};1.9)]>[3.0;449\ \mathrm{nm}(\mathbf{D3};2.1)]>[2.6;451\ \mathrm{nm}(\mathbf{D4};2.7)] \quad (8)$$

This inequality indicates that the pyridone azo dyes, including a quinolone azo dye, exhibited photosensitivity-noticeable fading in the mixture dyeings with **E1**. In inequality (8) dyes **D5** and **D1** showed a more marked tendency. Two dyes with low photosensitivity, **D3** and **D4**, can be added to the inequality (7). Pyridone azo dyes, which show little spectral overlap with **E1**, have a photosensitization-noticeable effect on the experimental/theoretical $k_{0,\mathrm{Yellow}}/k_{0,\mathrm{E1}}$ values.

In this case, however, fair sharing of the $^1O_2$ generated by the component dyes seemed not to occur; the rate of fading for **E1** was suppressed to a greater extent than that of its partner dyes. Thus in the mixture dyeings of **E1**, two effects were observed: a spectral overlap effect by red and orange dyes and a photosensitization-noticeable effect by yellow dyes with high sensitivity. Dye **A3**, however, exhibited a smaller spectral superposition effect than for the case of mixture dyeing with **E1** as shown in Table 6 (see Sec. 3.3.3 for **C1**).

For dye **B3**, with the same tendency as inequality (7), the photosensitization of **E1** was considerably suppressed due to the spectral overlap of this dye with the $\lambda_{\max}$ of 457 nm, resulting in a decrease in the generation of $^1O_2$. The K/S spectra of mixture dyeings with these two dyes exhibited practically no fading upon exposure for 80 h. Since dye **B3** possessed a very small f_i value in nature, the decrease in the generation of $^1O_2$ caused a large decrease in the oxidative fading of **B3**, as demonstrated by the small ratio of $(k_{0,\mathrm{Yellow}}/k_{0,\mathrm{E1}})_{\mathrm{Exp}}/(k_{0,\mathrm{Yellow}}/k_{0,\mathrm{E1}})_{\mathrm{MO}}$. In these mixture dyeings, dye **E1** exhibited also a very little fading.

By mixing **E1** with violet, red, orange, and/or yellow dyes with very small f_i values, which cause effective partial shielding of the sensitivity of **E1**, one can made a disperse dye mixture with a very high LF.

Thus, although the observed $k_{0,i}/k_{0,\mathrm{E1}}$ values for mixture dyeings with **E1** can be interpreted as above, the validity of the estimation of $k_{0,i}$ values by the MO method is appropriately confirmed. The $(k_{0,\mathrm{Yellow}}/k_{0,\mathrm{E1}})_{\mathrm{Exp}}/(k_{0,\mathrm{Yellow}}/k_{0,\mathrm{E1}})_{\mathrm{MO}}$ values was shifted by the spectral overlap between component dyes and their photosensitivity, although their behaviors was further explained below.

3.3.3. Combination dyeings with *C1*

As illustrated in Table 1, the seven dyes used exhibited larger K_{PET} and $k_{0,i}/k_{0,\mathrm{R1}}$ values than those of **R1**, although each single dye among the eight dyes examined showed exceptional behavior in its K_{PET} and $k_{0,i}/k_{0,\mathrm{R1}}$ values. Since dye **C1** possesses a very small $k_{0,i}/k_{0,\mathrm{R1}}$ value and a large f_i/f_{R1} value, it may exert catalytic fading action on its partner dyes, if the spectral overlap between the component dyes is not considerable.

In the mixture dyeings of **C1**, dyes **D1**, **D4**, **D7**, and **D2** exhibited lower rates of fading compared with single dyeings. As a result, the experimental $k_{0,\mathrm{Yellow}}/k_{0,\mathrm{C1}}$ values for the first two dyes were smaller than the theoretical values estimated by the PM5 method, while **D2** exhibited an experimental value quite similar to the theoretical one. In the mixture dyeing with **D7**, the observed $k_{0,\mathrm{Yellow}}/k_{0,\mathrm{C1}}$ value was much larger than the theoretical one.

When the same ratios, $(k_{0,\mathrm{Yellow}}/k_{0,\mathrm{C1}})_{\mathrm{Exp}}/(k_{0,\mathrm{Yellow}}/k_{0,\mathrm{C1}})_{\mathrm{MO}}$; $\lambda_{\max}$ (partner dye(s); f_i/f_{R1}), as those for dye **E1** are estimated for this case, they become as follows:

$$\left[(k_{0,\mathrm{Yellow}}/k_{0,\mathrm{C1}})_{\mathrm{Exp}}/(k_{0,\mathrm{yellow}}/k_{0,\mathrm{C1}})_{\mathrm{MO}};\lambda_{\max}(\text{partner dye(s)};f_i/f_{\mathrm{R1}})\right] : [2.7;421\ \mathrm{nm}(\mathbf{D7};27)] > [1.1;437\ \mathrm{nm}(\mathbf{D2};3.8)]>[0.77;451\ \mathrm{nm}(\mathbf{D4};2.7)]\approx[0.77;434\ \mathrm{nm}(\mathbf{D1};1.9)]. \quad (9)$$

No effect of spectral overlapping can be recognized but rather a dominant effect by the f_i/f_{R1} values of the partner dyes is seen. Depending upon the f_i/f_{R1} values of the partner dyes in the mixture dyeings with **C1**, the experimental $k_{0,\mathrm{Yellow}}/k_{0,\mathrm{C1}}$ values became larger or smaller than the theoretical values. This tendency is the same as the case of mixture dyeing of **E1** with the pyridone azo dyes [1,2], although the photosensitization-noticeable effect in the mixture dyeing was much smaller for **C1** than for **E1**.

From the difference in the effect of **D4** exhibited in the fading behavior of mixture dyeings of **C1** compared to **E1**, it can be inferred that little spectral overlapping effect occurred in the mixture dyeing of **C1**, although a considerable apparent improvement in LF of the partner dyes was recognized. Dye **C1**, irrespective of its larger f_i/f_{R1} value, may be used more safely in mixture dyeing as the blue component than **E1**, although the essential reason for this is debatable. As discussed in the next section, an apparent increasing tendency the in $(k_{0,\mathrm{Yellow}}/k_{0,\mathrm{C1}})_{\mathrm{Exp}}/(k_{0,\mathrm{Yellow}}/k_{0,\mathrm{C1}})_{\mathrm{MO}}$ ratios is attributed to the nitro group combined with activating group. Due to the lack of the latter group, dye C1 exhibited little or no increasing tendency.

3.3.4. General fading behavior of component dyes in mixture dyeings

The fading behaviors of **A3**, **E1**, and **C1** exhibited in the mixture dyeings can be interpreted in terms of the two essential parameters, $k_{0,i}/k_{0,\mathrm{R1}}$ and f_i/f_{R1}, being influenced by the mutual spectral overlap between the component dyes and the f_i/f_{R1} value of the partner dye, although the specific properties of the spectral overlapping or differences in the effects between the blue dyes remain to be characterized.

When the same calculation for the mixture dyeings previously reported [2] was performed, the results were as follows:

For **D2**, $\left[(k_{0,\mathrm{D2}}/k_{0,\mathrm{Blue}})_{\mathrm{Exp}}/(k_{0,\mathrm{D2}}/k_{0,\mathrm{Blue}})_{\mathrm{MO}};(\text{Blue dye})\right]$: $[4.5(\mathbf{E1})]>[4.2(\mathbf{E2})]>[2.8(\mathbf{R1})]>[2.0(\mathbf{E3})]>[1.3(\mathbf{E4})]>[1.1(\mathbf{C1})]>[0.94(\mathbf{A3})]$. (10)

For **D1**, $\left[(k_{0,\mathrm{D1}}/k_{0,\mathrm{Blue}})_{\mathrm{Exp}}/(k_{0,\mathrm{D1}}/k_{0,\mathrm{Blue}})_{\mathrm{MO}};(\text{Blue dye})\right]$: $[4.2;(\mathbf{E1})]>[1.7(\mathbf{R1})]>[1.5(\mathbf{E2})]>[0.86(\mathbf{E3})]>[0.80(\mathbf{E4})]>[0.77(\mathbf{C1})]\approx[0.77(\mathbf{A3})]$. (11)

Although the reversion of **R1** and **E2** in inequalities (10) and (11) cannot be explained, the order of blue and red dyes in promoting the fading of the partner dyes becomes:

$$\mathbf{E1} > \mathbf{E2} \approx \mathbf{R1} > \mathbf{E3} > \mathbf{E4} > \mathbf{C1} > \mathbf{A3}. \quad (12)$$

In inequality (12), dyes **R1** and **E2** are placed at the same position (cf. Sec. 3.3.3 for the reversal between inequality (10) and (11)). Although the order of **E2**, **R1**, and **E3** in suppressing the fading of the partner dye may not be interpreted, these dyes can be used as component dyes in mixture dyeing with yellow, orange or red dyes as exemplified by inequalities (10) and (11).

One of the possible interpretations of the differences in the effects of dyes **E1** and **C1** may be the base line spectra in the wavelength region below 450 nm (cf. Fig. 4). Dye **E1** is almost transparent in the region, while the K/S spectrum of **C1** possesses a minimum at about 430–440 nm and increases gradually at both longer and shorter wavelengths on either side of the minimum. If the absorptions at shorter wavelengths shield the absorptions of the yellow dyes, the photosensitivity of the yellow dyes may be suppressed to a considerable extent.

The $k_{0,i}/k_{C1}$ value for **C1** is about a quarter of the corresponding value, $k_{0,i}/k_{E1}$, for **E1**. Dye **C1** in the mixture dyeings seems to suppress the photosensitivity of yellow partner dyes by a factor of ca. 5 compared to **E1**. Dyes **C1** and **A3** seem to suppress the photosensitivity of yellow partner dyes similarly.

In the single dyeings, the fading behaviors of disperse dyes on PET on exposure to light in air could be exhibited by two parameters: $k_{0,i}/k_{0,R1}$ and f_i/f_{R1}, while in the mixture dyeings, the $(k_{0,i}/k_{0,Blue})_{Exp}/(k_{0,i}/k_{0,Blue})_{MO}$ ratios (where blue denotes primary component, blue, red etc. of combination dyeing) became usually more than unity, although in some cases less than unity. The spectral overlap of component dyes and an increase in the total dye concentration in PET (since the concentration of oxygen in PET is limited) may be primary factors to increase the ratios. Since no $k_{0,i}/k_{0,R1}$ values should change with the combination, the apparent increasing tendency of $(k_{0,i}/k_{0,Blue})_{Exp}/(k_{0,i}/k_{0,Blue})_{MO}$ ratios may be primarily attributed to a decrease in the fading of primary component. The closer the λ_{max} of the partner dye to that of red or blue dye or the larger the spectral overlap, the ratios became larger. This fact may cause an apparent decrease in the photosensitivity of primary component.

In addition to the apparent decreasing effect in photosensitivity, the apparent tendency to promote the fading of partner dyes expressed by inequality (12) was recognized. The largest promoting tendency of **E1** followed by **E2** and **E3** and least by **A3** without nitro group, may indicate the effect of nitro groups (whose absorption may exist in the UV-A region) together with activation by cyano and second nitro groups [3], although the tendency is further debatable.

In the mixture dyeing of blue and red dyes with partner dyes having MAB of shorter wavelengths, the fading of the partner dyes occurred faster than that of the component dyes of deeper hue. For binary mixture dyeings, the rate of fading for either dye was faster than that in the single dyeings, if this is defined as catalytic fading, we can observe no catalytic fading in the present study. If catalytic fading is defined as the fading of either dye whose rate was considerably faster than that of the other dye, a marked off-tone fading, we can find many examples of catalytic fading.

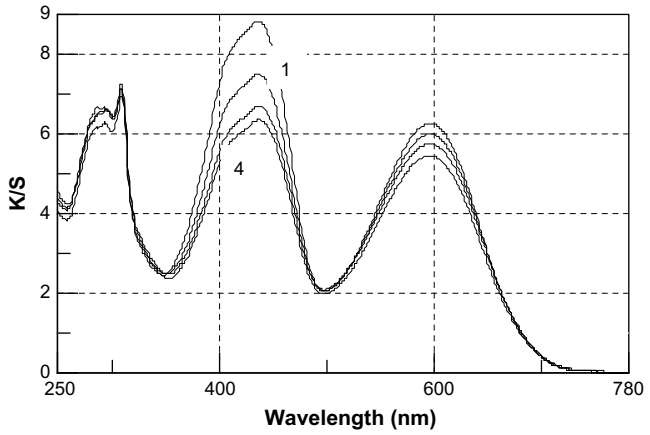

Fig. 4. K/S spectra of mixture-dyed PET with dyes **C1** and **D2** on exposure to a carbon arc for: 1, 0 h; 2, 20 h; 3, 40 h and 4, 60 h. (Spectra 2 and 3 (from top to bottom) in sequence are illustrated between 1 and 4.).

4. Summary

The photofading of eight disperse azo dyes, phenylazo-N,N-bis(ethanol)anilines, phenylazo-N-ethanolanilines, phenylazo-indoles and hetarylazo-anilines, on PET was analyzed by measuring the reflectance spectra (250–780 nm) of light exposed samples. The $k_{0,i}$ values were estimated using the linear relationship between the $S''_{m,n}(E)$ values and ln $k_{0,i}$ and then the relative values of $k_{0,i}/k_{R1}$ were obtained. The $S''_{m,n}(E)$ values were estimated by frontier orbital theory. Based on the hypothesis of a linear relationship between K_{PET} and the product of $k_{0,i}$ and f_i, the relative values of f_i/f_{R1} were experimentally determined.

Dye **B3** has the smallest f_i/f_{R1} value among the dyes and excellent LF (super LF dye) irrespective of having a considerably large $k_{0,i}/k_{R1}$ value. Dyes **B1** and **B2** have $k_{0,i}/k_{R1}$ values larger than that of **B3** and exhibit almost the same LF on PET. Dye **B2** exhibits good LF because it has the next smallest f_i/f_{R1} value among the eight dyes examined, while **B1** has a fair LF due to the larger f_i/f_{R1} value than that of **R1**. Dye **C1** has the smallest $k_{0,i}/k_{R1}$ and rather large f_i/f_{R1} value among the eight dyes (This dye is suitable for use as a blue component because, if partner dyes with small f_i/f_{R1} value are used, they shield partially the MAB of **C1** so as to lower the photosensitivity.) Dyes **A1**, **A2** and **A3** have both the $k_{0,i}/k_{R1}$ and f_i/f_{R1} values considerably larger than that of **R1**. These phenylazo-N-(ethanol)aniline dyes with scarlet to red hue have low LF comparable with pyridone azo dyes, which are not used as dyes for PET. In order to design azo dyes with excellent LF on PET, values of $k_{0,i}$ and f_i lower than those of **R1** are required.

Utilizing the mutually photosensitized fading in the mixture dyeings the validity of $k_{0,i}$ values estimated by the MO method was checked. The mixture dyeing of **A3** with the yellow dyes demonstrated the validity of $k_{0,i}/k_{R1}$ values estimated by the MO method, although it suppressed the fading of partner dyes depending upon the spectral overlap. The mixture dyeing of **C1** with yellow dyes demonstrated also the validity of $k_{0,i}/k_{R1}$ values, but it suppresses the fading of partner dyes.

When the combination was ideal, partner dyes with small f_i/f_{R1} values were used, which showed mutual spectral overlap so as to lower the photosensitivity of the main component with deeper hue, and the fading of component dyes in the mixture dyeings is considerably improved. The mixture dyeing of **E1** indicated large deviations from the theoretical $k_{0,Yellow}/k_{E1}$ values due to little spectral overlapping or little shielding by **E1**, but the fading of **E1** was suppressed only in exceptional cases such as in mixture dyeings with **B3**.

References

[1] Okada Y, Hihara T, Morita Z. Analysis of the catalytic fading of pyridone-azo disperse dyes on polyester using the semi-empirical, molecular orbital PM5 method. Dyes and Pigments 2008;78(3):179–98.
[2] Okada Y, Hihara T, Morita Z. Analyses of the photofading of phenylazo-aniline and phenylazo-pyridone disperse dyes on poly(ethylene terephthalate)

substrate using the semiempirical molecular orbital PM5 method. Dyes and Pigments 2008;79(2):111–25.
[3] Okada Y, Hihara T, Morita Z. Photo-fading for phenylazo-aniline, -pyridone and -quinolone disperse dyes on a nylon 6 substrate. Coloration Technology 2009;125(2):86–98.
[4] Müller C. Recent developments in the chemistry of disperse dyes and their intermediates. American Dyestuff Reporter 1970;59(3):37–44.
[5] Kitao T, Watada Y, Matsuoka M, Konishi K. Contribution of nitro group on the anomalous photofading of some azo disperse dyes. Nihon Kagaku Kaishi 1974;4:757–61.
[6] Matsuoka M, Seko H, Sugimoto T, Yutani S, Kitao T, Konishi K. Photofading of disperse azo dyes. Kogyo Kagaku Zasshi 1971;74(8):1655–60.
[7] Freeman HS, Hsu WN. Photolytic behavior of some popular disperse dyes on polyester and nylon substrates. Textile Research Journal 1987;57(4):223–34.
[8] Iesce MR, Cermola F, Temussi F. Photooxygenation of heterocycles. Current Organic Chemistry 2005;9(2):109–39.
[9] Hihara T, Okada Y, Morita Z. Photo-oxidation and -reduction of vat dyes on water-swollen cellulose and their lightfastness on dry cellulose. Dyes and Pigments 2002;53(2):153–77.
[10] Hihara T, Okada Y, Morita Z. Photo-oxidation of pyrazolinylazo dyes and analysis of reactivity as azo and hydrazone tautomers using semiempirical molecular orbital PM5 method. Dyes and Pigments 2006;69(2):151–76.
[11] Hihara T, Okada Y, Morita Z. The photo-oxidation of reactive azobenzene dyes and an analysis of the reactivity as the azo and hydrazone tautomers using the PM5 method. Dyes and Pigments 2007;75(1):225–45.
[12] Hihara T, Okada Y, Morita Z. A semiempirical molecular orbital study on the photo-reactivity of monoazo reactive dyes derived from γ- and J-acids. Dyes and Pigments 2007;73(2):141–61.
[13] Hihara T, Okada Y, Morita Z. An analysis of the photo-reactivity of monoazo reactive dyes derived from H-acid and related naphthalene sulfonic acids using the PM5 method. Dyes and Pigments 2007;75(3):585–605.
[14] Hihara T, Okada Y, Morita Z. Reactivity of phenylazonaphthol sulfonates, their estimation by semiempirical molecular orbital PM5 method, and the relation between their reactivity and azo-hydrazone tautomerism. Dyes and Pigments 2003;59(3):201–22.
[15] Hihara T, Okada Y, Morita Z. Relationship between photochemical properties and colourfastness due to light-related effects on monoazo reactive dyes derived from H-acid, γ-acid, and related naphthalene sulfonic acids. Dyes and Pigments 2004;60(1):23–48.
[16] Fukui K,, Fujimoto H, editors. Frontier orbitals and reaction paths, selected papers of Fukui K. World Scientific Series in 20th Century Chemistry, vol. 7. Singapore: World Scientific; 1997.
[17] Fukui K, Yonezawa T, Shingu H. A molecular orbital theory of reactivity in aromatic hydrocarbons. Journal of Chemical Physics 1952;20(4):722–5.
[18] Fukui K, Yonezawa T, Nagata C, Shingu H. Molecular orbital theory of orientation in aromatic, heteroaromatic and other conjugated molecules. Journal of Chemical Physics 1954;22(8):1433–42.
[19] Fukui K, Yonezawa T, Nagata C. Interrelations of quantum-mechanical quantities concerning chemical reactivity of conjugated molecules. Journal of Chemical Physics 1957;26(4):831–41.